Relevance of the iron-responsive element (IRE) pseudotriloop structure for IRP1/2 binding and validation of IRE-like structures using the yeast three-hybrid system

Chen, S.C.; Olsthoorn, R.C.L.

Gene 710 (2019) 399–405

Contents lists available at ScienceDirect

Gene

journal homepage: www.elsevier.com/locate/gene

Research paper

Relevance of the iron-responsive element (IRE) pseudotriloop structure for IRP1/2 binding and validation of IRE-like structures using the yeast three-hybrid system

Shih-Cheng Chen[1], René C.L. Olsthoorn*

Leiden Institute of Chemistry, Leiden University, Leiden, the Netherlands

ARTICLE INFO

Keywords:
Pseudotriloop
Iron-responsive element
RNA structure
Iron-regulatory protein, RNA-protein interaction
Yeast three-hybrid system

ABSTRACT

Iron-responsive elements (IREs) are ~35-nucleotide (nt) stem-loop RNA structures located in 5′ or 3′ untranslated regions (UTRs) of mRNAs that mediate post-transcriptional regulation by their association with IRE-binding proteins (IRPs). IREs are characterized by their apical 6-nt loop motif 5'-CAGWGH-3′ (W = A or U and H = A, C or U), the so-called pseudotriloop, of which the loop nts C1 and G5 are paired, and the none-paired C between the two stem regions. In this study, the yeast three-hybrid (Y3H) system was used to investigate the relevance of the pseudotriloop structure of ferritin light chain (FTL) for the IRE-IRP interaction and the binding affinities between variant IRE(-like) structures and the two IRP isoforms, IRP1 and 2. Destabilization of the pseudotriloop structure by a G5-to-A mutation reduced binding of IRP1 and 2, while restoring the pseudotriloop conformation by the compensatory C1-to-U mutation, restored binding to both IRPs. In particular, IRP1 showed even stronger binding to the C1U-G5A mutant than to the wildtype FTL IRE. On the other hand, deletion of the bulged-out U6 of the pseudotriloop did not significantly affect its binding to either IRP1 or 2, but substitution with C particularly enhanced the binding to IRP1. In comparison to FTL IRE, IRE-like structures of 5′-aminolevulinate synthase 2 (ALAS2) and *SLC40A1* (also known as ferroportin-1) showed similar or, in the case of endothelial PAS domain protein 1 (EPAS1) IRE, slightly weaker binding affinity to IRPs. *SLC11A2* (a.k.a. divalent metal transporter-1) IRE exhibited relatively weak binding to IRP1 and medium binding to IRP2. Notably, the IRE-like structure of α-synuclein showed no detectable binding to either IRP under the conditions used in this Y3H assay. Our results indicate that Y3H can be used to characterize binding between IRPs and various IRE-like structures *in vivo*.

1. Introduction

Iron (Fe^{2+}) is involved in multiple cellular processes, including respiration, DNA synthesis, oxygen transport, energy metabolism, *etc.*, and hence its cellular homeostasis is precisely regulated in most organisms. In vertebrates, the cellular iron level is stably maintained within a narrow range to avoid damage to protein, DNA, and lipid, as an excess or deficiency of cellular iron may lead to physiological misregulation, *e.g.* abnormal cell proliferation. In humans, impaired iron homeostasis is associated with inherited hemochromatosis, cirrhosis, cardiomyopathy, diabetes mellitus, and many neurodegenerative disorders, *e.g.* Friedreich's ataxia, Parkinson's and Alzheimer's diseases (Madsen and Gitlin, 2007; Simmons et al., 2007; Fleming and Ponka, 2012). The uptake of cellular iron is predominantly accomplished by divalent metal transporter 1 (DMT1, encoded by *SLC11A2*) and transferrin receptor (TfR1), while the storage and sequestration of cellular iron is mediated by H- and L-ferritin subunits (HTL and FTL), and the export and translocation of cellular iron is facilitated by the basolateral exporter ferroportin (encoded by *SLC40A1*). All these actions are tightly controlled to regulate cellular iron homeostasis (reviewed in (Anderson et al., 2012)).

The key regulator of intracellular iron metabolism is iron-regulatory protein (IRP), a member of the aconitase superfamily that post-transcriptionally regulates many genes involved in iron metabolism by

Abbreviations: IRE, iron-responsive element; IRP, iron binding protein; PTL, pseudo-triloop; Y3H, yeast three-hybrid; FTL, ferritin light chain; UTR, untranslated region; ALAS2, 5′-aminolevulinate synthase 2; EPAS1, endothelial PAS domain protein 1; TfR1, transferrin receptor; DMT1, divalent metal transporter 1; Wt, wild type; PCR, polymerase chain reaction; 3-AT, 3-Amino-1,2,4-triazole

* Corresponding author.
E-mail addresses: scchen@kmu.edu.tw (S.-C. Chen), olsthoor@chem.leidenuniv.nl (R.C.L. Olsthoorn).
[1] Current address: Office of Research and Development, Kaohsiung Medical University, Kaohsiung, Taiwan.

https://doi.org/10.1016/j.gene.2019.06.012
Received 1 May 2019; Received in revised form 16 May 2019; Accepted 6 June 2019
Available online 12 June 2019

specifically binding to the conserved iron-responsive elements (IREs) located in the UTRs of mRNAs (Hentze et al., 2004; Wallander et al., 2006; Wilkinson and Pantopoulos, 2014; Zhang et al., 2014). For instance, when Fe^{2+} levels are low, IRPs are able to tightly bind to IRE(s) present in the 3' UTR of the TfR1 mRNA to stabilize the transcripts and increase the protein level of TfR1 that promotes iron uptake. On the other hand, low Fe^{2+} levels also facilitate IRPs to interact with IREs located in the 5' UTR of *SLC40A1* mRNA and reduce the protein level of the iron-exporting Ferroportin. As a result, the iron-sensing IRP-IRE interaction increases the uptake and the availability of iron in cells. On the contrary, high Fe^{2+} levels decrease IRP's IRE-binding affinity, resulting in reduced stability of TfR1 mRNA and increased translation of *SLC40A1* mRNA that synergistically depletes cellular iron (Cairo et al., 2006). Thus, knowledge of IRE binding affinity is key to the study of IRP-mediated iron homeostasis (Rouault, 2006; Zhang et al., 2014).

The sequence and structure of IREs are highly conserved in mammalians, and generally consist of a stem-loop element formed by a five base pair stem carrying a 6-nucleotide (nt) apical loop motif 5′-CAGWGH-3′ (W = A or U and H = A, C or U) separated from a lower stem of variable length by an internal loop or bulge containing a conserved C (Wallander et al., 2006; Leipuviene and Theil, 2007; Muckenthaler et al., 2008; Volz, 2008). Since the classic IREs have been identified in ferritin mRNA (Aziz and Munro, 1987; Hentze et al., 1987), quite a few IRE-like structures have been proposed later in other mRNAs, of which the encoded proteins are not necessarily solely involved in iron homeostasis, *e.g.* 5′-aminolevulinate synthase 2 (ALAS2, a.k.a. eALAS), endothelial PAS domain protein 1 (EPAS1), and α-synuclein (Friedlich et al., 2007; Sanchez et al., 2007; Rogers et al., 2011; Sanchez et al., 2011; Febbraro et al., 2012). Some of these RNA elements, discovered by immunoprecipitation, were demonstrated to have IRP binding affinity *in vitro* using electrophoretic mobility shift assays (EMSA) (Dandekar et al., 1991; Wilkinson and Pantopoulos, 2014), whereas those predicted by computational analysis, *e.g.* the IRE-like structure found in α-synuclein mRNA 5' UTR, have not been reported for direct binding to IRPs, although their involvement in transcriptional regulation have been reported (Ma et al., 2012).

In this study, we took advantage of the yeast three-hybrid (Y3H) system (Putz et al., 1996; SenGupta et al., 1996) which has been broadly used to assay RNA-protein interaction *in vivo* (Jaeger et al., 2004b; Hook et al., 2005) to study the relevance of the pseudotriloop conformation of the FTL IRE for binding to IRP1 and 2. Furthermore, we also validated the binding potentials of several IRE-like structures to the two IRP isoforms in Y3H system.

2. Materials and methods

2.1. Constructs of RNA and protein expressing vectors for yeast three-hybrid system

The Y3H system used in this study is generally adapted from what has been reported (SenGupta et al., 1996). The wildtype FTL (FTL-wt) IRE is taken as a standard IRE in this study, of which the apical loop consists of 5'-CAGUGU-3′. IRE mutants and variants were constructed by cloning complementary pairs of chemically synthesized DNA oligonucleotides (Eurogentec, Belgium) into NheI/BglII digested pIIIA/MS2.1*, a modified version of pIIIA/MS2.1 (Jaeger et al., 2004a) in which the unique SmaI and the flanking redundant sequences were removed by replacing the fragment between the two EcoRI sites with the sequence 5′-aatttatactcacatgaggatcacccatgtaattaacactgaggatcaccc-cagtggctagcttctagaaagatctg-3′ thereby creating unique NheI, XbaI, and BglII sites downstream of the MS2 CP binding sequences (Chen and Olsthoorn, 2010). Additional nucleotides were introduced at the bottom of the lower stem of the IREs (indicated in Fig. 4a) that stabilize the RNA structure in order to minimize the potential formation of alternative structures. The RNA-binding protein expressing vector was based on the shuttle vector pGADT7 (Clontech, USA) and constructed as described previously (Chen and Olsthoorn, 2010). DNA fragments encoding IRP1 and 2 were generated by PCR and inserted between SmaI and XhoI sites of pGADT7, in frame with the GAL4 domain at the C-terminus.

2.2. Yeast three-hybrid assay

The pIIIA/MS2.1-IREs, vectors that produce the chimeric RNA of IRE and MS2 Coat protein (CP) binding sequence, and the pGADT7-IRPs, vectors that express the IRP-GAL4 fusion protein were co-introduced to yeast strain L40-coat which expresses the MS2-CP-LexA fusion protein (SenGupta et al., 1996). Transformed yeast cells inheriting both vectors were cultured on selective medium. To assay the reporter of RNA-protein interaction, HIS3 expression, we monitored the phenotypic growth of transformed yeast L40 coat on 3-Amino-1,2,4-triazole (3-AT) containing Yeast Nitrogen Base (YNB) medium as described previously (Haeger, 2004; Chen and Olsthoorn, 2010). Briefly, three independent colonies of L40-coat yeast which were transformed simultaneously with pIIIA/MS2.1-IREs and pGADT7-IRPs were cultured 2 days in Leu^-, Ade^-, and Ura^- YNB medium at 30 °C. The yeasts were then sub-cultured, in 1-to-1000 ratio, to an optical density of ~0.2 at 600 nm, followed by applying 2 μl onto Leu^-, Ade^-, Ura^-, and His^- YNB agar containing 0 to 15 mM 3-AT. After culturing for 4 days at 30 °C, the phenotypic growth of two represented clones was documented.

3. Results

3.1. Binding affinity between IREs and IRPs in yeast three-hybrid system

The RNA baits, FTL-wt IRE and its mutants, and the protein preys, IRP1 and 2, were cloned into expression vectors for Y3H assay, respectively (Fig. 1, adapted from SenGupta et al. (SenGupta et al., 1996)). Each mutant of FTL IRE (Fig. 2a) was co-transformed to yeast strain L40-Coat with either IRP1 or IRP2 expressing vectors to study the IRE-IRP interaction in yeast. The binding affinity between the tested IREs and IRPs was evaluated by the phenotypic growth of the yeast on HIS^- media, as binding between the bait and the prey leads to transactivation of the reporter gene HIS3 (SenGupta et al., 1996; Jaeger et al., 2004b; Jaeger et al., 2004a), enabling the transformed yeast to

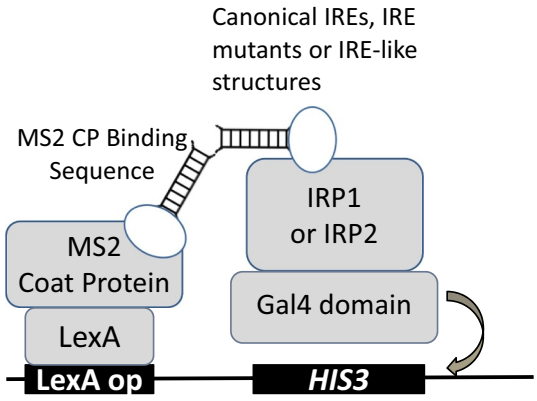

Fig. 1. The yeast three-hybrid (Y3H) system to assay binding affinity between IRE and IRP1 and 2. The principle components of the Y3H system used in this study are shown, including (i) the hook, fusion protein consisting of LexA DNA-binding domain and MS2 coat protein (CP), (ii) the bait, a chimeric RNA structure consists of MS2 CP binding sequence and IRE, IRE mutants or IRE-like structures, (iii) the fish, transcriptional activation domain Gal4 fused to IRP1 or 2. The transcriptional activation of the reporter gene HIS3 only occurs upon sufficient RNA-protein interaction between the tested IRE and the IRP that completes the formation of the trimeric complex (illustration adapted form (SenGupta et al., 1996)).

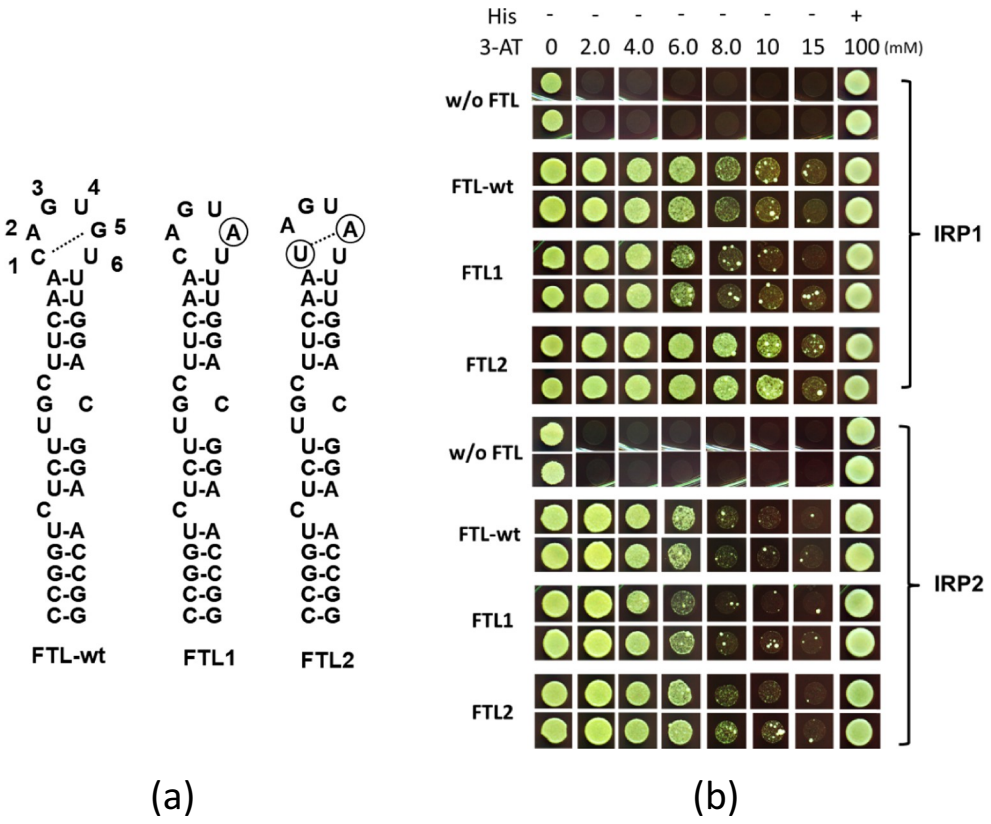

Fig. 2. Yeast three-hybrid assay to verify the relevance of the pseudotriloop base pairing of the IRE to the binding with IRP1 and 2. (a) The secondary structures of the IRE of ferritin light chain (FTL-wt) and the pseudotriloop mutants FTL1-2 are shown. Base substitutions are marked with a circle. The dotted-line represents the intra-loop base pairing of the pseudotriloop. (b) In the yeast assay, higher resistance to 3-AT represents a stronger RNA-protein interaction. "w/o FTL" is the negative control of which the RNA ligand has no chimeric IRE element, while clones FTL1 and FTL2 contain mutated IRE elements. The upper panel displays the binding affinities between the tested FTL IRE/mutants and IRP1 while the lower panel shows the binding to IRP2, respectively.

grow on media without histidine supplementation.

In Y3H assays, non-specific RNA-protein/protein-protein interaction and/or promoter leakage may lead to background HIS3 expression. Therefore, 3-AT is usually added to the medium to eliminate false-positive RNA-protein interaction in Y3H system. In our study of IRE-IRP interaction, yeast possessing solely MS2-coat binding sequence without the RNA bait IRE, showed false positive growth on selective medium without 3-AT when the vector expressing either IRP1 or 2 was co-transformed (Fig. 2b). However, addition of 2 mM of 3-AT could completely suppress such false positive growth and can be considered as the threshold for specific IRE-IRP interactions in the following tests. IRP1 shows strong binding affinity to FTL-wt IRE, exhibiting good growth on the media containing 3-AT up to 6 mM (Fig. 2b). A similar growth pattern was observed for IRP2 (Fig. 2b), suggesting that IRP2 and IRP1 have similar binding affinity for the wildtype FTL IRE.

3.2. Relevance of the IRE pseudotriloop structure to IRP binding affinity

One of the structurally conserved features of the IRP binding IRE is the C1:G5 intra-loop base pairing (Fig. 2a), making the apical loop a classic example of pseudotriloop (Henderson et al., 1994; Sierzputowska-Gracz et al., 1995). We have studied the importance of the C1:G5 base pairing for IRE-IRP binding in yeast by evaluating the binding affinity between the G5A mutant FTL1 and IRPs (Fig. 2b). The result indicated that disruption of this intra-loop base-pairing reduced the binding to IRP1 as shown by the lowered 3-AT resistance (Fig. 2b). Interestingly, restoration of the pseudotriloop by the compensatory C1U mutation (mutant FTL2) significantly increased binding of IRP1 relative to FTL-wt IRE as indicated by sustained growth at 10 mM 3-AT (Fig. 2b). Binding of IRP2 was less influenced by the pseudotriloop conformation as disruption (FTL1) and restoration (FTL2) of the intra-loop base pair slightly reduced and increased growth respectively, relative to FTL-wt (Fig. 2b).

3.3. Relevance of U6 and G3 in IRE pseudotriloop for IRP binding

Four additional mutants of FTL IRE were constructed to investigate the role of conserved bases within the 5'-CAGWGH-3′ motif for binding to IRP1 and 2, respectively (Fig. 3). Deletion of U6 (mutant FTL3) seemed to increase binding affinity to IRP1 in one data set but not in the other (Fig. 3b), so at best we can conclude that deletion of U6 has no detrimental effect on IRP1 binding in Y3H. Replacing U6 with C (mutant FTL4) did increase binding affinity (Fig. 3b). Substitution of G3 by U either with (mutant FTL6) or without (mutant FTL5) an additional U6G mutation merely resulted in slightly lower binding of IRP1 relative to FTL-wt IRE (Fig. 3b). IRP2 was rather insensitive to deletion of U6 (FTL3) and mutations in the loop (FTL5 and 6) but showed on average stronger binding to the U6C mutant (Fig. 3c, FTL4).

3.4. Validation of the binding between IRE-like structures and IRPs

Several recently identified IRE-like structures (Fig. 4) were validated for their binding affinity to IRPs in Y3H, including the IREs of EPAS1, α-synuclein, SLC40A1, ALAS2, and SLC11A2 mRNAs. All these RNA structures exhibit the characteristic features of an IRE (Fig. 4a). Fig. 4b shows that IRP1 binds strongly to the IRE-like structures of SLC40A1, EPAS1, and ALAS2 and weakly to the IRE-like structures of SLC11A2, whereas the interaction between IRP1 and the proposed IRE of α-synuclein is below the detection threshold set for a specific RNA-protein interaction in Y3H. Compared to FTL-wt IRE, IRP1 binds to SLC40A1 and EPAS1 IREs with similar affinity, and to SLC11A2 IRE with lower affinity. Although the variation between the datasets of ALAS2 is high, binding of IRP1 is on average similar to FTL-wt. We conclude that IRE-like structures having a relatively stable 5-basepair upper stem tend to interact with IRP1 with similar affinity as FTL IRE, whereas structures with a thermodynamically unstable upper stem, e.g. IREs of SLC11A2, bind weaker to IRP1 in Y3H system. A similar trend of binding was found between these IRE-like structures and IRP2 as well,

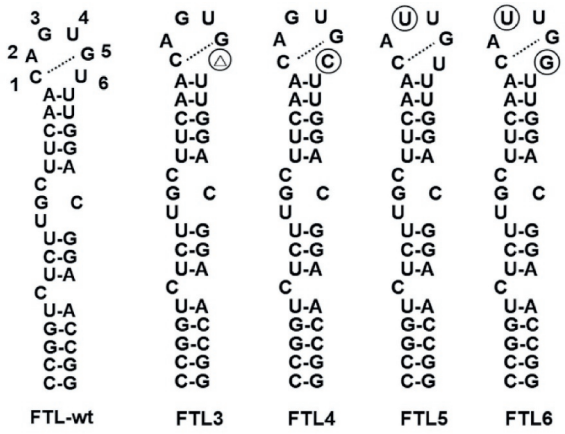

(a)

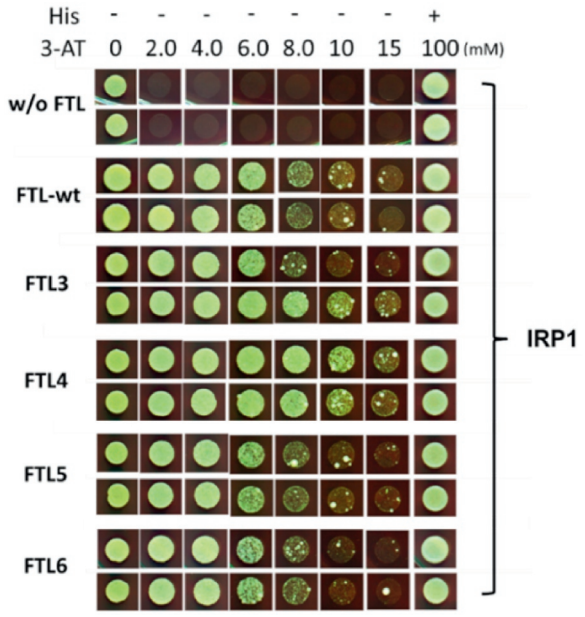

(b)

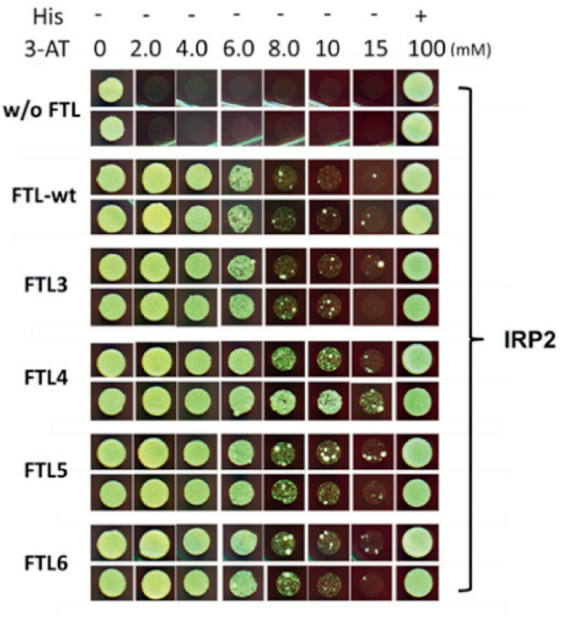

(c)

Fig. 3. Yeast three-hybrid assay to verify the relevance of G3 and U6 of the IRE to the binding with IRP1 and 2. (a) The secondary structures of the IRE of ferritin light chain (FTL-wt) and the mutants tested (FTL3-6) are shown. Base substitutions are marked with a circle while base deletions are marked with a triangle. The dotted-line represents the intra-loop base pairing of the pseudotriloop. (b) The binding affinities between IRE mutants FTL3 to 6 and IRP1 were assayed by Y3H system, respectively. Clone w/o FTL is the negative control of which the RNA ligand has no IRE structure, while clones FTL3 to 6 contain mutated IRE elements. (c) The binding affinities between IRE mutants FTL3 to 6 and IRP2 were assayed by Y3H system, respectively.

except that IRP2 bound to SLC11A2 IRE more strongly than IRP1 did (Fig. 4c).

4. Discussion

4.1. Insights in binding affinities between IRPs and variant IRE-like structures in vivo

In the studies of IRP-IRE complex reported previously, two large and spatially separate domains of IRP1 have been shown to bind to the IRE, which predominantly form 10 bonds with the AGU pseudotriloop and 8 bonds with the inter-stem C- bulge (Walden et al., 2006; Volz, 2008), suggesting that the pseudotriloop and the C-bulge of IREs are the critical binding sites for IRP1. All the IRE variants studied in this study exhibit such a characteristic AGU pseudotriloop and the C-bulge (Fig. 4a), but their binding affinities for IRPs were found differ in Y3H system. For instance, IRP1 and 2 interact with EPAS1 and ALAS2 IREs as strongly as with FTL IRE, whereas the interactions with *SCL11A2* and α-synuclein IREs are much weaker than FTL IRE (Fig. 4b). Thus, the presence of the apical AGU sequence and the bulged C is not a guarantee for strong binding to IRPs. Notably, although the IRE-like structure located in the 5'UTR of α-synuclein mRNA (Friedlich et al., 2007; Febbraro et al., 2012) has been reported to play a role in regulating the expression of α-synuclein (Rogers et al., 2011; Mikkilineni et al., 2012; Bandyopadhyay et al., 2013), its direct binding to IRPs is substantially weaker than other tested IRE-like structures and cannot be distinguish from non-specific RNA-protein interaction in Y3H (Fig. 4). This result is in agreement with the previously reported inability to identify IRPs

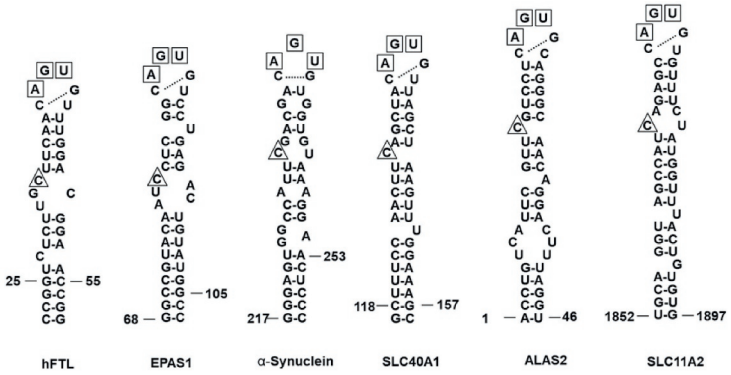

(a)

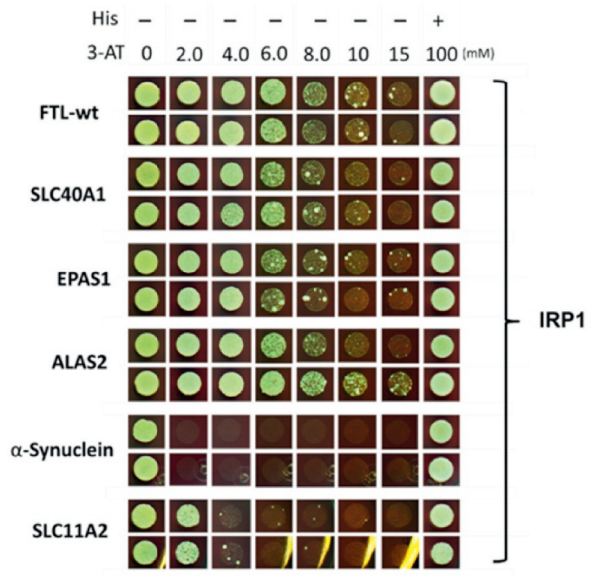

(b)

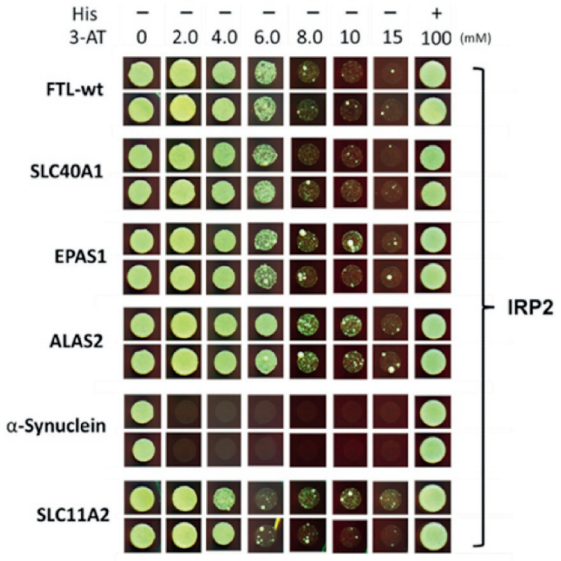

(c)

Fig. 4. Variant IREs studied in yeast three-hybrid system. (a) Secondary structures of ferritin light chain (FTL) IRE (Aziz and Munro, 1987), SLC40A1 IRE (Lymboussaki et al., 2003), endothelial PAS domain protein 1 (EPAS1) IRE (Sanchez et al., 2007), α-synuclein IRE (Friedlich et al., 2007), 5′-aminolevulinate synthase 2 (ALAS2) IRE (Dandekar et al., 1991), and *SLAC11A2* (Abboud and Haile, 2000) are shown. The highly conserved A, G, and U bases in the IRE pseudotriloop are boxed, and the numbering indicates the span of each element according to the reference mRNA sequences of each gene (Accession number NM_000146.4, NM_001430.5, NM_000345.3, NM_014585.5, NM_000032.5, NM_000617.2. Additional nucleotides were introduced into the lower stem region as indicated to stabilize the IRE structure. (b) Yeast three-hybrid assay to verify the binding affinity between variant IREs and IRP1 and (c) IRP2.

through RNA pulldown with the IRE-like structure of α-synuclein, as well as the failure to detect α-synuclein mRNA by protein pulldown with IRP1/2 (Sanchez et al., 2011; Koukouraki and Doxakis, 2016). Collectively, these data suggest that the iron-mediated translational regulation of α-synuclein mRNAs does not directly or solely rely on IRP-IRE interactions but mediated by a more complex mechanism.

4.2. Differential binding affinities between the IRP1/2 and variant IREs

Of the two IRP isoforms, IRP1 functions both as an RNA-binding protein and as the cytosolic aconitase, while IRP2 functions solely as an RNA-binding protein. It has been proposed that IRP1 is the major iron sensor and IRE binder as the abundance of IRP1 is higher than that of IRP2 in most cells (Hentze and Kuhn, 1996). However, it is IRP2 that was found to dominate the regulation of mammalian iron homeostasis and control the expression of TfR1 and ALAS2 mRNAs (Meyron-Holtz et al., 2004a; Meyron-Holtz et al., 2004b; Wilkinson and Pantopoulos, 2014). Recently, IRP1 and 2 were found to regulate, respectively and/or collaboratively, different cellular mechanisms of iron metabolism, tumorigenesis, and neurodegeneration (Cho et al., 2010; Maffettone et al., 2010; Wang et al., 2014). In Y3H system, we have found that the differences in IRP1 and 2 to bind the canonical IREs, *e.g.* FTL and *SLC40A1* IREs, were not significant. This is in agreement with the data of Allerson et al. (Allerson et al., 1999) showing that FTL IRE constructs bind to IRP1 and 2 equally well in gel-shift assays. However, with respect to certain non-canonical IRE-like structures and mutants, *e.g. SLC11A2* IRE and the C1U:G5A mutant (FTL2) tested in this study, IRP1 and 2 did show differential binding affinities *in vivo*. Recently, cellular mRNAs that exclusively associated with IRP1 or IRP2 were identified with immunoprecipitation (Sanchez et al., 2011). These results implied

that the two isoforms of IRP, to a certain extent, can selectively regulate the expression of different subsets of mRNA in cells, depending on their binding preference to the variant IREs. The functional relevance of such selectivity may be of great interest in the future.

4.3. Interpretation of the IRE-IRP interaction in vivo

Recently, Khan et al. (Khan et al., 2017) reported that the kinetic and thermodynamic properties of ferritin and mitochondrial aconitase IRE-IRP1 interaction *in vitro* is affected by temperature and the presence of Mn^{2+}. This observation suggests that *in vitro* and *in vivo* RNA-protein binding assays, *e.g.* EMSA and Y3H, may lead to different conclusions due to their specific binding conditions. For example, Goforth et al., (Goforth et al., 2010) reported that IRP1 binding affinities for EPAS1 and ALAS2 IREs were 3.0 and 6.3 fold lower than that for the FTL IRE, respectively. However, we did not observe such binding differences in Y3H system *in vivo* (Fig. 4). Also, Gunshin et al. have shown using gel-shift assays that IRP1 binds to the 30-nt DMT1 IRE with a higher affinity compared to IRP2 (Gunshin et al., 2001), whereas here we showed in Y3H system that the 46-nt ALAS2 IRE (which differs from DMT1 only by an additional 16-nt lower stem) is preferentially bound by IRP2 (Fig. 4). These findings suggest that the length of the IRE hairpins could make a substantial difference in their binding affinities to IRP1 and 2. Considering that most IREs are part of a much longer mRNA *in vivo* the use of short RNA probes in gel-shift assays *in vitro* may not represent the actual situation. In this respect, an *in vivo* system such as Y3H involving larger RNAs and other proteins and nucleic acids comes closer to the actual conditions under which these IREs operate.

Altogether, our data show that the Y3H system can be used to compare binding affinities of IRPs between canonical IREs and various IRE-like structures in a semi-quantitative manner *in vivo*.

Funding

This research was supported by a VIDI grant from the Netherlands Organization for Scientific Research (NWO) awarded to R.C.L.O.

Conflicts of interest

The authors declare no conflict of interest.

References

Abboud, S., Haile, D.J., 2000. A novel mammalian iron-regulated protein involved in intracellular iron metabolism. J. Biol. Chem. 275, 19906–19912.
Allerson, C.R., Cazzola, M., Rouault, T.A., 1999. Clinical severity and thermodynamic effects of iron-responsive element mutations in hereditary hyperferritinemia-cataract syndrome. J. Biol. Chem. 274, 26439–26447.
Anderson, C.P., Shen, M., Eisenstein, R.S., Leibold, E.A., 2012. Mammalian iron metabolism and its control by iron regulatory proteins. Biochim. Biophys. Acta 1823, 1468–1483.
Aziz, N., Munro, H.N., 1987. Iron regulates ferritin mRNA translation through a segment of its 5′ untranslated region. Proc. Natl. Acad. Sci. U. S. A. 84, 8478–8482.
Bandyopadhyay, S., Cahill, C., Balleidier, A., Huang, C., Lahiri, D.K., Huang, X., Rogers, J.T., 2013. Novel 5′ untranslated region directed blockers of iron-regulatory protein-1 dependent amyloid precursor protein translation: implications for down syndrome and Alzheimer's disease. PLoS One 8, e65978.
Cairo, G., Bernuzzi, F., Recalcati, S., 2006. A precious metal: Iron, an essential nutrient for all cells. Genes Nutr. 1, 25–39.
Chen, S.C., Olsthoorn, R.C., 2010. In vitro and in vivo studies of the RNA conformational switch in alfalfa mosaic virus. J. Virol. 84, 1423–1429.
Cho, H.H., Cahill, C.M., Vanderburg, C.R., Scherzer, C.R., Wang, B., Huang, X., Rogers, J.T., 2010. Selective translational control of the Alzheimer amyloid precursor protein transcript by iron regulatory protein-1. J. Biol. Chem. 285, 31217–31232.
Dandekar, T., Stripecke, R., Gray, N.K., Goossen, B., Constable, A., Johansson, H.E., Hentze, M.W., 1991. Identification of a novel iron-responsive element in murine and human erythroid delta-aminolevulinic acid synthase mRNA. EMBO J. 10, 1903–1909.
Febbraro, F., Giorgi, M., Caldarola, S., Loreni, F., Romero-Ramos, M., 2012. alpha-Synuclein expression is modulated at the translational level by iron. Neuroreport 23, 576–580.
Fleming, R.E., Ponka, P., 2012. Iron overload in human disease. N. Engl. J. Med. 366, 348–359.
Friedlich, A.L., Tanzi, R.E., Rogers, J.T., 2007. The 5′-untranslated region of Parkinson's disease alpha-synuclein messengerRNA contains a predicted iron responsive element. Mol. Psychiatry 12, 222–223.
Goforth, J.B., Anderson, S.A., Nizzi, C.P., Eisenstein, R.S., 2010. Multiple determinants within iron-responsive elements dictate iron regulatory protein binding and regulatory hierarchy. RNA 16, 154–169.
Gunshin, H., Allerson, C.R., Polycarpou-Schwarz, M., Rofts, A., Rogers, J.T., Kishi, F., Hentze, M.W., Rouault, T.A., Andrews, N.C., Hediger, M.A., 2001. Iron-dependent regulation of the divalent metal ion transporter. FEBS Lett. 509, 309–316.
Haeger, R.S., 2004. How technology has transformed the one-visit initial exam. J Clin Orthod 38, 425–434.
Henderson, B.R., Menotti, E., Bonnard, C., Kuhn, L.C., 1994. Optimal sequence and structure of iron-responsive elements. Selection of RNA stem-loops with high affinity for iron regulatory factor. J. Biol. Chem. 269, 17481–17489.
Hentze, M.W., Kuhn, L.C., 1996. Molecular control of vertebrate iron metabolism: mRNA-based regulatory circuits operated by iron, nitric oxide, and oxidative stress. Proc. Natl. Acad. Sci. U. S. A. 93, 8175–8182.
Hentze, M.W., Caughman, S.W., Rouault, T.A., Barriocanal, J.G., Dancis, A., Harford, J.B., Klausner, R.D., 1987. Identification of the iron-responsive element for the translational regulation of human ferritin mRNA. Science 238, 1570–1573.
Hentze, M.W., Muckenthaler, M.U., Andrews, N.C., 2004. Balancing acts: molecular control of mammalian iron metabolism. Cell 117, 285–297.
Hook, B., Bernstein, D., Zhang, B., Wickens, M., 2005. RNA-protein interactions in the yeast three-hybrid system: affinity, sensitivity, and enhanced library screening. RNA 11, 227–233.
Jaeger, S., Eriani, G., Martin, F., 2004a. Critical residues for RNA discrimination of the histone hairpin binding protein (HBP) investigated by the yeast three-hybrid system. FEBS Lett. 556, 265–270.
Jaeger, S., Eriani, G., Martin, F., 2004b. Results and prospects of the yeast three-hybrid system. FEBS Lett. 556, 7–12.
Khan, M.A., Walden, W.E., Theil, E.C., Goss, D.J., 2017. Thermodynamic and kinetic analyses of iron response element (IRE)-mRNA binding to Iron regulatory protein, IRP1. Sci. Rep. 7, 8532.
Koukouraki, P., Doxakis, E., 2016. Constitutive translation of human alpha-synuclein is mediated by the 5′-untranslated region. Open Biol. 6, 160022.
Leipuviene, R., Theil, E.C., 2007. The family of iron responsive RNA structures regulated by changes in cellular iron and oxygen. Cell. Mol. Life Sci. 64, 2945–2955.
Lymboussaki, A., Pignatti, E., Montosi, G., Garuti, C., Haile, D.J., Pietrangelo, A., 2003. The role of the iron responsive element in the control of ferroportin1/IREG1/MTP1 gene expression. J. Hepatol. 39, 710–715.
Ma, J., Haldar, S., Khan, M.A., Sharma, S.D., Merrick, W.C., Theil, E.C., Goss, D.J., 2012. Fe2+ binds iron responsive element-RNA, selectively changing protein-binding affinities and regulating mRNA repression and activation. Proc. Natl. Acad. Sci. U. S. A. 109, 8417–8422.
Madsen, E., Gitlin, J.D., 2007. Copper and iron disorders of the brain. Annu. Rev. Neurosci. 30, 317–337.
Maffettone, C., Chen, G., Drozdov, I., Ouzounis, C., Pantopoulos, K., 2010. Tumorigenic properties of iron regulatory protein 2 (IRP2) mediated by its specific 73-amino acids insert. PLoS One 5, e10163.
Meyron-Holtz, E.G., Ghosh, M.C., Iwai, K., LaVaute, T., Brazzolotto, X., Berger, U.V., Land, W., Ollivierre-Wilson, H., Grinberg, A., Love, P., Rouault, T.A., 2004a. Genetic ablations of iron regulatory proteins 1 and 2 reveal why iron regulatory protein 2 dominates iron homeostasis. EMBO J. 23, 386–395.
Meyron-Holtz, E.G., Ghosh, M.C., Rouault, T.A., 2004b. Mammalian tissue oxygen levels modulate iron-regulatory protein activities in vivo. Science 306, 2087–2090.
Mikkilineni, S., Cantuti-Castelvetri, I., Cahill, C.M., Balliedier, A., Greig, N.H., Rogers, J.T., 2012. The anticholinesterase phenserine and its enantiomer posiphen as 5'untranslated-region-directed translation blockers of the Parkinson's alpha synuclein expression. Parkinsons Dis 2012, 142372.
Muckenthaler, M.U., Galy, B., Hentze, M.W., 2008. Systemic iron homeostasis and the iron-responsive element/iron-regulatory protein (IRE/IRP) regulatory network. Annu. Rev. Nutr. 28, 197–213.
Putz, U., Skehel, P., Kuhl, D., 1996. A tri-hybrid system for the analysis and detection of RNA–protein interactions. Nucleic Acids Res. 24, 4838–4840.
Rogers, J.T., Mikkilineni, S., Cantuti-Castelvetri, I., Smith, D.H., Huang, X., Bandyopadhyay, S., Cahill, C.M., Maccecchini, M.L., Lahiri, D.K., Greig, N.H., 2011. The alpha-synuclein 5'untranslated region targeted translation blockers: anti-alpha synuclein efficacy of cardiac glycosides and Posiphen. J. Neural Transm. (Vienna) 118, 493–507.
Rouault, T.A., 2006. The role of iron regulatory proteins in mammalian iron homeostasis and disease. Nat. Chem. Biol. 2, 406–414.
Sanchez, M., Galy, B., Muckenthaler, M.U., Hentze, M.W., 2007. Iron-regulatory proteins limit hypoxia-inducible factor-2alpha expression in iron deficiency. Nat. Struct. Mol. Biol. 14, 420–426.
Sanchez, M., Galy, B., Schwanhaeusser, B., Blake, J., Bahr-Ivacevic, T., Benes, V., Selbach, M., Muckenthaler, M.U., Hentze, M.W., 2011. Iron regulatory protein-1 and -2: transcriptome-wide definition of binding mRNAs and shaping of the cellular proteome by iron regulatory proteins. Blood 118, e168–e179.
SenGupta, D.J., Zhang, B., Kraemer, B., Pochart, P., Fields, S., Wickens, M., 1996. A three-hybrid system to detect RNA-protein interactions in vivo. Proc. Natl. Acad. Sci. U. S. A. 93, 8496–8501.
Sierzputowska-Gracz, H., McKenzie, R.A., Theil, E.C., 1995. The importance of a single G in the hairpin loop of the iron responsive element (IRE) in ferritin mRNA for structure: an NMR spectroscopy study. Nucleic Acids Res. 23, 146–153.
Simmons, D.A., Casale, M., Alcon, B., Pham, N., Narayan, N., Lynch, G., 2007. Ferritin accumulation in dystrophic microglia is an early event in the development of

Huntington's disease. Glia 55, 1074–1084.
Volz, K., 2008. The functional duality of iron regulatory protein 1. Curr. Opin. Struct. Biol. 18, 106–111.
Walden, W.E., Selezneva, A.I., Dupuy, J., Volbeda, A., Fontecilla-Camps, J.C., Theil, E.C., Volz, K., 2006. Structure of dual function iron regulatory protein 1 complexed with ferritin IRE-RNA. Science 314, 1903–1908.
Wallander, M.L., Leibold, E.A., Eisenstein, R.S., 2006. Molecular control of vertebrate iron homeostasis by iron regulatory proteins. Biochim. Biophys. Acta 1763, 668–689.
Wang, W., Deng, Z., Hatcher, H., Miller, L.D., Di, X., Tesfay, L., Sui, G., D'Agostino Jr., R.B., Torti, F.M., Torti, S.V., 2014. IRP2 regulates breast tumor growth. Cancer Res. 74, 497–507.
Wilkinson, N., Pantopoulos, K., 2014. The IRP/IRE system in vivo: insights from mouse models. Front. Pharmacol. 5, 176.
Zhang, D.L., Ghosh, M.C., Rouault, T.A., 2014. The physiological functions of iron regulatory proteins in iron homeostasis - an update. Front. Pharmacol. 5, 124.